Analysis of T_e/T_i Effect on Confinement Properties*)

Emi NARITA[1)], Tomonori TAKIZUKA[1,2)], Nobuhiko HAYASHI[2)], Takaaki FUJITA[2)], Shunsuke IDE[2)], Mitsuru HONDA[2)], Akihiko ISAYAMA[2)], Kiyoshi ITAMI[2)], Yutaka KAMADA[2)], Yasuyuki TANAKA[1)], Masaki IIDA[1)] and Takeshi FUKUDA[1)]

[1)] *Graduate School of Engineering, Osaka University, Suita, Osaka 565-0871, Japan*

[2)] *Naka Fusion Institute, Japan Atomic Energy Agency, Naka, Ibaraki 311-0193, Japan*

(Received 9 December 2011 / Accepted 31 May 2012)

In order to improve the prediction capability of confinement properties in burning plasmas with intensive electron heating, we have re-visited the DB3v10 International H-mode Confinement Database with emphasis on the temperature ratio T_e/T_i and considerations on kinetic profiles. It was thereby found that the impact of T_e/T_i is more apparent for discharges with peaked density profiles. Namely, H_H factor improves with an increase of peakedness in the density profile for $T_e/T_i < 1$, whereas it tends to deteriorate with the density peaking for $T_e/T_i > 1$. The confinement scaling with a contribution of T_e/T_i was also elaborated. In addition, the influence of T_e/T_i described above was examined qualitatively with GS2 and GLF23 codes, which provided results corroborating the performed regression analysis, indicating the interplay of ITG and TEM in the turbulence transport.

Keywords: H-mode, burning plasma, confinement scaling law, T_e/T_i ratio, GS2, GLF23, ITG, TEM

DOI: 10.1585/pfr.7.2403102

1. Introduction

It is doubtless that scaling expressions for the thermal energy confinement carry a significant role in fusion research. Amongst them, the most well-known and established is IPB98(y,2) [1], which was elaborated based on the international H-mode database compiled under the ITPA framework and applied to ITER predictions. Although the database is enormous, being composed of global confinement data from 19 tokamaks in the world, a large fraction of the discharges are dominantly ion-heated. On the other hand, it is pointed out that electron heating substantially degrades the high performance discharges [2]. In particular, an intensive electron heating by fusion alphas is anticipated in burning plasmas [3]. Hence, the utmost objective of our work is to resolve the underlying physics pertaining to the influence of electron heating and quantitatively define the influence of T_e/T_i on the confinement, in order to improve the prediction capability for ITER and fusion reactors. Here, profile effects have also been incorporated, as they are regarded prerequisite [1, 4], and we thus aim to establish a confinement scaling with considerations of the profile effect.

The international H-mode confinement database has been revisited, and the influence of T_e/T_i on the confinement in the database has been examined. In addition to the regression analysis using the database, simulation analysis using GS2 [5] and GLF23 [6] models have been undertaken. Comparison of simulation results with the database-analysis results has been made to understand the effects of T_e/T_i and density peakedness on the turbulent transport and confinement performance.

2. Evidence of T_e/T_i Effect and Profile Contributions in Global Confinement Database

We have firstly extracted 317 data from JET and 81 data from ASDEX Upgrade (AUG), out of the DB3v10 H-mode Database [1, 7] i.e., no transport barriers inside. Several data of AUG are corrected a little [8]. The percentage of the points in $T_{e0}/T_{i0} < 1$ region is 68%. Here, subscript '0' represents the quantities evaluated at the plasma center. The major discharge parameters therein considered are as follows. In data from JET, $1.5 < I_p[\mathrm{MA}] < 5.1$, $1.2 < B_t[\mathrm{T}] < 3.8$, $1.1 < n_{eL}[10^{19}\,\mathrm{m^{-3}}] < 5.6$, $2.8 < q_{95} < 5.7$, $1.5 < \kappa_a < 1.8$, and $0.29 < \delta < 0.58$, and in data from AUG, $0.59 < I_p[\mathrm{MA}] < 1.3$, $1.5 < B_t[\mathrm{T}] < 3.1$, $3.3 < n_{eL}\ [10^{19}\,\mathrm{m^{-3}}] < 9.7$, $3.0 < q_{95} < 6.9$, $1.5 < \kappa_a < 1.7$, and $0.10 < \delta < 0.29$. Here, I_p, B_t, n_{eL}, q_{95}, κ_a and δ are plasma current, toroidal magnetic field, line average electron density, safety factor at 95% flux surface, ellipticity, and triangularity, respectively. The range of T_{e0}/T_{i0} is $0.5 < T_{e0}/T_{i0} < 1.5$, and the density range was limited below 60% of Greenwald density $n_{GW}[10^{20}\mathrm{m^{-3}}] = I_p/\pi a^2[\mathrm{MAm^{-2}}]$, in order to avoid concerns other than the transport. Based on the results of JT-60U experiments reported in Ref. 2, we have intuitively divided the whole data into two groups of different peakedness in the density pro-

author's e-mail: narita@ppl.eng.osaka-u.ac.jp

*) This article is based on the presentation at the 21st International Toki Conference (ITC21).

file; one in the range $1.0 < n_{e0}/n_{eL} < 1.1$ and the other in $1.1 < n_{e0}/n_{eL} < 1.6$. Namely, the electron density profile is flat in the first group and peaked in the second group. We have derived the following two scaling laws for the thermal energy confinement time τ_{sc} according to the range of n_{e0}/n_{eL} [9]

$$\tau_{sc1} = 0.0808 I_p^{0.91} B_t^{0.11} n_{eL}^{0.28} P_L^{-0.59} R^{1.73} M^{0.27} \varepsilon^{0.54} \kappa_a^{0.41} \quad : 1.0 < n_{e0}/n_{eL} < 1.1, \tag{1}$$

$$\tau_{sc2} = 0.0653 I_p^{0.90} B_t^{0.08} n_{eL}^{0.34} P_L^{-0.63} R^{1.78} M^{0.16} \varepsilon^{0.41} \kappa_a^{0.72} \quad : 1.1 < n_{e0}/n_{eL} < 1.6. \tag{2}$$

Here, units and notations are τ_{sc}[s], I_p[MA], B_t[T], $n_{eL}[10^{19}\,\mathrm{m}^{-3}]$, P_L:loss power[MW], R:major radius[m], M:ion mass number, and ε:inverse aspect ratio. Although the difference in exponent for each variable is small from the IPB98(y,2) scaling, the standard deviations σ ($\sigma^2 = N^{-1}\Sigma(\tau_{th}/\tau_{sc} - 1)^2$, here N is the number of points, and τ_{th} is the thermal energy confinement time) are reduced in comparison with the IPB98(y,2) base: the value of σ for the flat density profile case has been reduced from 0.104 to 0.102, and that for the peaked density case has been reduced from 0.178 to 0.167. It is known that the peaking factor in density profiles plays an important role in anomalous transport induced by microinstabilities. In addition, T_e/T_i is considered to be a crucial quantity related to the dynamics pertaining to ion temperature gradient (ITG) mode, electron temperature gradient (ETG) mode and trapped electron mode (TEM). Figure 1 shows histograms of τ_{th}/τ_{sc1} (flat density case) and τ_{th}/τ_{sc2} (peaked density case) for $T_{e0}/T_{i0} < 1$ and $T_{e0}/T_{i0} > 1$. For discharges with $T_{e0}/T_{i0} < 1$, the number of points with large τ_{th}/τ_{sc2} increases in the peaked density case (Fig. 1 (c)) by comparison with the flat density case (Fig. 1 (a)), and therefore the peaked density profile improves the confinement for $T_{e0}/T_{i0} < 1$. On the other hand in the case of $T_{e0}/T_{i0} > 1$, the peaked density profile degrades the confinement, since the number of points with small τ_{th}/τ_{sc2} increase in the peaked density case (Fig. 1 (d)). These indicate that T_{e0}/T_{i0} dependence is more prominent in the peaked density case. Keep in mind there also exist the small number of improved confinement data even for $T_{e0}/T_{i0} > 1$. We will discuss about these data in section 3 and 5.

3. Scaling Expression Including T_e/T_i Term and its Implications on Active Microinstabilities

Having a rudimentary insight on the possible role of T_{e0}/T_{i0} on the confinement, we have elaborated a scaling law that incorporates the T_{e0}/T_{i0} term. We treat the data of peaked density discharges, because of their clear variation against T_e/T_i as shown in the previous section. Besides the T_e/T_i ratio other nondimensional variables [10], namely $(B_t R^{1.25})$, $(n_{eL}/n_{GW}*) = (n_{eL}/n_{GW}) \times (0.5/a)^{0.25}$ and $q = 2.5(1+\kappa_a^2)(B_t a^2/RI_p)$ are taken in. The figure of merit

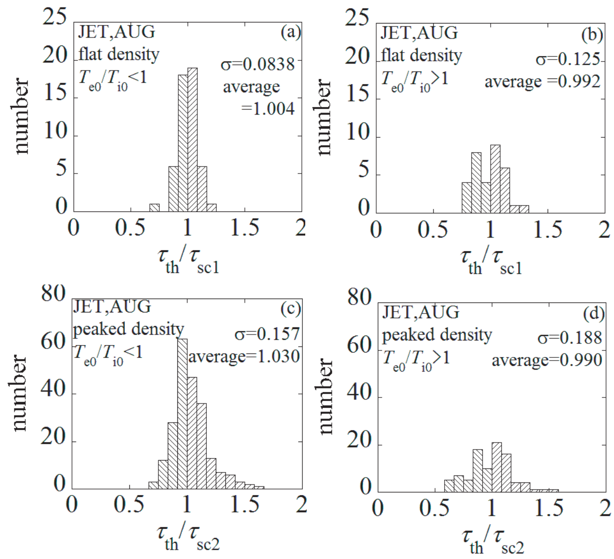

Fig. 1 Histograms of τ_{th}/τ_{sc1} for flat density case (upper row), and those of τ_{th}/τ_{sc2} for peaked density case (lower row). $T_{e0}/T_{i0} < 1$ data are shown in (a) and (c). $T_{e0}/T_{i0} > 1$ data are shown in (b) and (d).

related to the enhancement in confinement was defined as $(\tau_{th}/\tau_{sc2} - 1)/(T_{e0}/T_{i0} - 1)$, and we assumed that it is written in a form $(\tau_{th}/\tau_{sc2} - 1)/(T_{e0}/T_{i0} - 1) = \mathrm{C} \times (B_t R^{1.25})^{\alpha} \times (n_{eL}/n_{GW}*)^{\beta} \times q^{\gamma}$. Next, the database was divided into two regions (A): $(\tau_{th}/\tau_{sc2} - 1)/(T_{e0}/T_{i0} - 1) < 0$ and (B): $(\tau_{th}/\tau_{sc2} - 1)/(T_{e0}/T_{i0} - 1) > 0$. In (A) range, the increase in T_{e0}/T_{i0} leads deterioration of thermal confinement, on the other hand, in (B) range, the confinement is improved even for $T_{e0}/T_{i0} > 1$. The dependences on $n_{eL}/n_{GW}*$ and q were weak, and the following confinement expressions have been heuristically obtained in each range [9]:

$$\tau_{sc3} = \tau_{sc2} \times \{1 - 0.157 \times (T_{e0}/T_{i0} - 1) \times (B_t R^{1.25})^{0.59}\} \quad : (\tau_{th}/\tau_{sc2} - 1)/(T_{e0}/T_{i0} - 1) < 0, \tag{3}$$

$$\tau_{sc4} = \tau_{sc2} \times \{1 + 0.913 \times (T_{e0}/T_{i0} - 1) \times (B_t R^{1.25})^{-0.81}\} \quad : (\tau_{th}/\tau_{sc2} - 1)/(T_{e0}/T_{i0} - 1) > 0. \tag{4}$$

The derived scaling was applied to the database from AUG and JET, and the fitting result is shown in Fig. 2 where the standard deviation σ is 0.132. The exclusion of T_{e0}/T_{i0} term increased the value of σ to 0.167, whereas RMSE for IPB98(y,2) is 15.6%. This result suggests that in both (A) and (B) ranges, the T_{e0}/T_{i0} dependences are found.

Since the effect of T_{e0}/T_{i0} is remarkable in peaked-density discharges, we have next examined the effect of n_{e0}/n_{eL} for the (A) region. The correcting term $f = -0.157 \times (T_{e0}/T_{i0} - 1) \times (B_t R^{1.25})^{0.59}$ in Eq. (3) was plotted against n_{e0}/n_{eL} in Fig. 3. We find that the peaked density profiles contribute to an improvement of confinement for the ion heating cases i.e., in low value of T_{e0}/T_{i0} range, while the peaked density profiles degrade the confinement in high value of T_{e0}/T_{i0} range. Dedicated experiments to

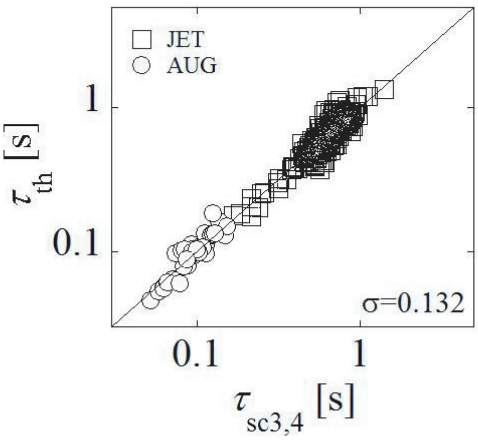

Fig. 2 Fitted data on scaling laws indicated in Eqs. (3) and (4) that include the contributions of T_{e0}/T_{i0} for peaked density discharges.

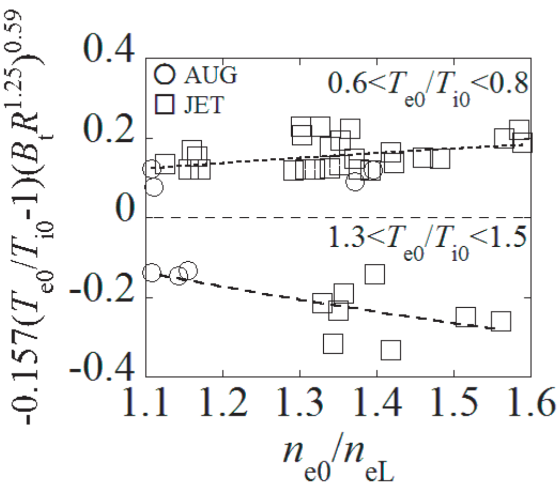

Fig. 3 Dependence of the correction term of the scaling law indicated in Eq. (3) on n_{e0}/n_{eL} for high and low values of temperature ratio.

investigate into the influence of electron heating in AUG also corroborated the regression results performed in our work [11].

4. Qualitative Validation of Regression Results with Gyrokinetic Code and Transport Model

GS2 and GLF23 calculations have been undertaken, in order to validate the above regression results and to understand the related physics behind. The GS2 code [5] is a gyrokinetic code that resolves low-frequency turbulence in magnetized plasmas, and it is widely used to assess the microinstability of plasmas in a variety of configurations. Linear and quasilinear properties of the fastest growing mode at several prescribed wavenumbers have been calculated independently in our work, as mentioned below.

Figure 4 shows the results of linear GS2 runs under the

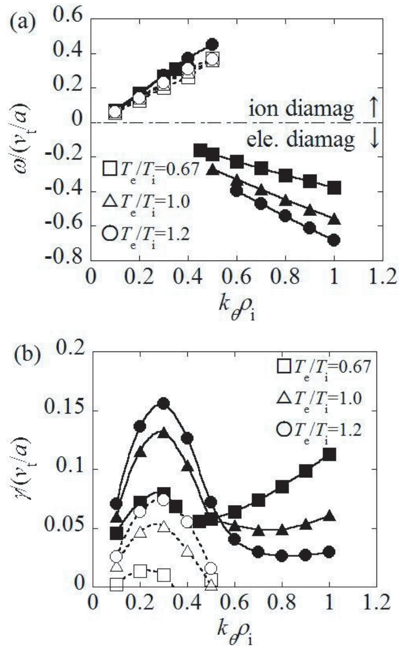

Fig. 4 Results of GS2 linear analysis: (a) normalized real frequency and (b) normalized linear growth rate as functions of normalized wave number. Non adiabatic case (solid symbol) is compared with adiabatic-electron case (open symbol) for various temperature ratio, T_e/T_i = 0.67 (□), 1.0 (Δ) and 1.2 (○).

adiabatic-electron case and the nonadiabatic case. Equilibrium option of the "*s-alpha* model" for low-β plasma [5] was employed with the representative parameters: R/a = 2.7, r/a = 0.5, q = 1.7 and s = 0.84. Here r is the minor radius, and s is the magnetic shear. The normalized density and temperature gradients were chosen as R/L_n = 3.0 and R/L_{Ti} = R/L_{Te} = 5.5. In practice, the range of $0.1 < k_\theta\rho_i < 1.0$ corresponding to ITG/TEM modes has been examined. Here, k_θ is the wave number in the poloidal direction and ρ_i is the ion Larmor radius. The real frequency ω and the growth rate γ are normalized to v_t/a where $v_t = (T_i/m_i)^{0.5}$. The influence of flow shear has not been considered for simplicity. Figure 4 (a) shows the wave-number dependence of normalized real frequency of the fastest growing mode, where negative (positive) real frequency indicates the propagation in the electron (ion) diamagnetic direction in accordance with the output from GS2 calculation. The dominant instability changes from ITG mode to TEM at $k_\theta\rho_i$ = 0.5 for the nonadiabatic case. Figure 4 (b) illustrates that the normalized growth rate increases with the value of T_e/T_i for $k_\theta\rho_i < 0.5$. This trend of T_e/T_i dependence agrees well with the regression analysis result for the (A) range. The effect of kinetic electrons has been examined by comparing the results for the nonadiabatic case and those for the adiabatic-electron case. The kinetic electrons enhance the growth rate for $k_\theta\rho_i < 0.5$. Thus, not only ITG turbulence but also ITG/TEM turbulence can degrade the thermal confinement further with an increase in T_e/T_i. On the other hand, for $k_\theta\rho_i > 0.5$, TEM

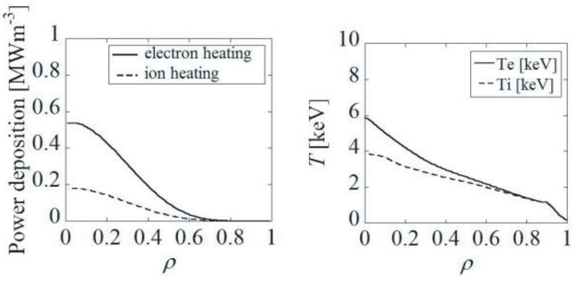

Fig. 5 Examples of (a) auxiliary heating profile and (b) the temperature profiles as results of the heating profiles. Here, density peaking factor n_{e0}/n_{eL} is 1.21.

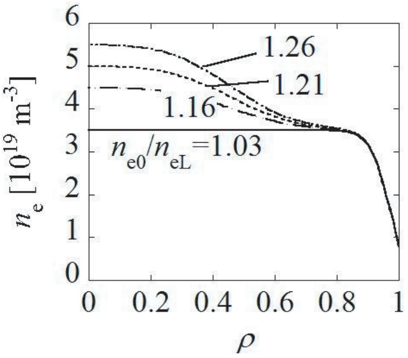

Fig. 6 Electron density profiles used for simulation with GLF23.

is destabilized with a decrease in T_e/T_i. The relation to the confinement property is to be studied in future.

Next the GLF23 transport model module was implemented in the transport code TOPICS [12], and transport simulations have been performed to compare with the results of regression analysis and GS2 calculation. GLF23 model [6] was originally developed to predict the core temperature profiles in tokamaks, and it is reported that the estimated growth rates of turbulence agree well with gyrokinetic linear stability codes.

The geometry as well as the anticipated parameters for JT-60SA has been herein chosen. The major discharge parameters are I_p = 2.3 MA, B_t =1.7 T, q_{95} = 4.7, κ = 1.9 and δ = 0.49. At ρ = 0.5, q = 1.7 and s = 0.84 as the same as is the calculation with GS2. The value of T_{e0}/T_{i0} is varied by changing the ratio between heating power deposition for electrons and ions. Examples of auxiliary heating profiles and the temperature profiles are shown in Fig. 5. The dependence of H_H factor on T_{e0}/T_{i0} in four different density profiles has been investigated. Here, H_H factor is defined as $H_H = \tau_{th}/\tau_{IPB98(y,2)}$. The density profile is fixed during a simulation run as shown in Fig. 6. The normalized density gradient R/L_n is 3.1 at ρ = 0.5 for the density profile with n_{e0}/n_{eL} = 1.26. The influences of alpha stabilization and $E \times B$ shear stabilization [6] are included. The alpha stabilization decreases a little H_H factor for the positive magnetic shear plasma, while the $E \times B$ shear stabilization works to slightly increase H_H factor. Figure 7 indicates

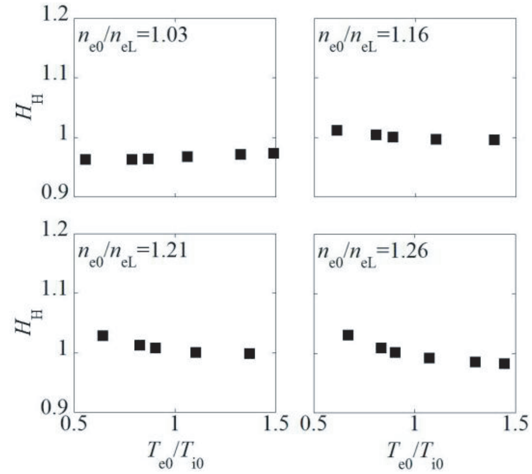

Fig. 7 H_H factor against T_{e0}/T_{i0} calculated by GLF23 in different density profiles.

that there is little T_{e0}/T_{i0} dependence for the flat density profile, as the same as in the regression analysis. With an increase in density peaking factor, the effect of T_{e0}/T_{i0} becomes prominent, and the increase in T_{e0}/T_{i0} deteriorates the thermal energy confinement. This result agrees with the trend of T_e/T_i dependence (A) in the regression analysis, and with the linear GS2 calculation.

5. Conclusions and Discussions

The influence of T_e/T_i was investigated through the regression analysis, using the international H-mode database. As a consequence, it was suggested that for discharges with peaked density profiles, the thermal confinement deteriorate with the increase in T_{e0}/T_{i0}.

In addition to the regression analysis, the influence of T_e/T_i has been examined with GS2 and GLF23 codes. The numerical simulations using GS2 demonstrate the trend whereby the increase in T_e/T_i enhances ITG/TEM transport. In addition, the simulations with GLF23 shows that in the flat density profile case, the effect of T_e/T_i is obscure, whereas in the peaked density case, H_H factor decreases with an increase in T_e/T_i. For these reasons, both codes agree with the results from the regression analysis.

In section 2 and 3, the existence of the data improved confinement even for $T_e/T_i > 1$ has been suggested. We have found that the TEM instability for $k_\theta \rho_i > 0.5$ is suppressed by an increase in T_e/T_i. In a plasma where ITG mode would play a minor role in the transport, this effect of T_e/T_i on TEM could improve the confinement asT_e/T_i increases. The further work is required to explore the above speculation

[1] Progress in the ITER Physics Basis, Chapter 2: Plasma confinement and transport, Nucl. Fusion **47**, S18 (2007).
[2] S. Ide *et al.*, Nucl. Fusion **47**, 1499 (2007); H. Takenaga *et al.*, Nucl. Fusion **49**, 075012 (2009); D.E. Newman *et al.*, Phys. Plasmas **5**, 938 (1998).

[3] T.H. Stix, Plasma Phys. **14**, 367 (1972).
[4] O. Kardaun *et al.*, Fusion Energy 2000 (2000), ITERP/04.
[5] M. Kotschenreuther *et al.*, Comp. Phys. Comm. **88**, 128 (1995). Source program is downloaded from http://www.gs2.sourceforge.net/
[6] R. Waltz *et al.*, Phys. Plasmas **4**, 2482 (1997). Source program is downloaded from http://w3.pppl.gov/ntcc/GLF/
[7] The international global H-mode confinement database, http://efdasql.ipp.mpg.de/hmodepublic/
[8] F. Ryter, private communication.
[9] E. Narita *et al*., Proc. 38th EPS Conf., P2-121, Strasbourg, 27 June-1 July, 2011.
[10] T. Takizuka *et al.*, JAERI-Research 95-075 (1995).
[11] F. Ryter *et al.*, Plasma Phys. Control. Fusion **43**, A323 (2001).
[12] N. Hayashi and JT-60 Team, Phys. Plasmas **17**, 056112 (2010).